

## Approximation methods for the nuclear thermodynamic functions and their validity in a solvable model

Y. Alhassid and J. Zingman

*A. W. Wright Nuclear Structure Laboratory, Yale University, New Haven, Connecticut 06511*

(Received 21 July 1983; revised manuscript received 5 March 1984)

Methods which include the effect of mean-field fluctuations on the nuclear partition function and level density of hot nuclei are tested by applying them to a many-body system for which exact solutions are available, the Lipkin model. It is found that for finite systems fluctuation corrections to the mean field partition function and level density can be substantial, and especially so near a shape phase transition where these fluctuations smooth out discontinuities in the mean-field quantities. The model calculations suggest that only time-independent fluctuations are important at high temperatures or at high excitation energies. Moreover, even when fluctuations are restricted to a small set of constraints, a significant improvement over the mean-field calculations can result. This is thus a practical approximation since it requires only knowledge of the deformation free energy surfaces at finite temperature.

### I. INTRODUCTION

A heavy nucleus typically has a very large number of states at high excitation energies, since there are many ways in which these internal energies can be distributed among the many nuclear degrees of freedom. It is thus hopeless to look for a completely detailed description of nuclear states at these energies, either experimentally or theoretically. Instead, we should try to single out quantities which are the result of averaging over many states. One such quantity, for instance, is the level density at a given excitation energy. The level density is of great importance as it describes the statistical factor which enters into various transition rates according to the Fermi golden rule. Theoretical estimations of the level density are thus essential for calculations of statistical  $\gamma$ -cascade decay rates of highly excited nuclei, formation rates of compound nuclei, and so on.

The level density can be considered as the partition function of the microcanonical ensemble. However, that ensemble has a sharp energy and is described by a singular distribution function which is not in a convenient form for applying standard approximation methods. Instead, it is much easier to work in terms of a smooth distribution in which the energy is allowed to fluctuate. Such a distribution is represented by the canonical ensemble at a finite temperature  $T = \beta^{-1}$ . Its partition function  $Z(\beta)$  is then related to the level density  $\rho(E)$  by a Laplace transform

$$Z(\beta) = \int_0^\infty dE e^{-\beta E} \rho(E). \quad (1.1)$$

Thus, we are naturally led to consider nuclei at finite temperatures, whether or not such states can be achieved and detected experimentally. The finite temperature formalism is, of course, of much more direct physical interest in cases where it is proven possible to heat nuclei to finite temperature. Indeed, nuclei can be heated to relatively high excitation energies in deep inelastic heavy ion col-

lisions.<sup>1</sup> There is evidence that at least a partial equilibration takes place in such reactions,<sup>2</sup> to a temperature which is, roughly speaking, the average excitation energy per nucleon.

In thermodynamics, it is considered to be a *fundamental relation*<sup>3</sup> when the free energy

$$F(\beta) = -\beta^{-1} \ln Z(\beta) \quad (1.2)$$

is given in terms of the temperature. This means that it contains all the thermodynamic information about the system that we can possibly have. Our main interest is therefore in applying tractable approximations to (1.2).

Mean-field theories have had considerable success in describing ground-state ( $T=0$ ) energies of nuclei<sup>4</sup> and have been generalized to finite temperatures, where they result in the temperature-dependent Hartree-Fock.<sup>5,6</sup> Pairing effects can also be incorporated by the finite temperature Hartree-Fock-Bogolyubov approximation.<sup>7</sup> For temperatures above  $\sim 1$  MeV these effects are small and we shall not consider them.<sup>8</sup> While the mean-field theories have traditionally been approached by the variational principle, in recent years another method based on functional integral representation of the partition function has been advocated.<sup>9</sup> The mean-field free energy functional of the latter approach is more general than the variational one since it allows time-dependent solutions.

As in the  $T=0$  case, there can be *several* solutions to the mean-field equations, which are found by constructing the free energy surfaces obtained when certain constraints are imposed on the mass distribution of the nucleus. As the microscopic constrained Hartree-Fock calculations are quite complicated, especially for shapes which do not have an axial symmetry, it has been suggested that these surfaces be constructed by applying the Strutinsky shell corrections at finite temperature.<sup>10,11</sup> Constrained Hartree-Fock calculations<sup>12</sup> in which the axial quadrupole moment is constrained show that a nucleus which is de-

formed in its ground state will usually undergo a phase transition to a spherical shape as the temperature is raised above a certain value.

A phenomenological description of quadrupole shape transitions using the framework of the Landau theory is provided in Ref. 13. This reference addresses itself also to the important problem of fluctuations around the equilibrium shape on the nuclear partition function. Previous calculations of level densities, based on realistic single particle schemes,<sup>14</sup> neglected such fluctuations. There are two reasons for the inclusion of these fluctuations in the mean-field theory. The first is that, as opposed to a thermodynamical system, the number of nucleons is *finite* (of order 100), and the second and most important is that near the phase transition the fluctuations in the mean field are known to be large. While the fluctuations can be taken into account by the saddle point method when the system is far away from the transition temperature, this latter approximation fails near the critical point. The proper way to treat fluctuations in such a case was illustrated in Ref. 13 for a quadrupole shape transition. It is called the uniform approximation<sup>15,16</sup> since it can be applied near the transition temperature as well as far from it. This method becomes practical when the fluctuations in the mean-field configuration are restricted to the constraint directions only, since it does not require more information than is provided by the finite-temperature free energy surface.

The conditions for the validity of the above approximations are hard to formulate quantitatively. It is thus important to apply and test these methods in a many-body system which is also amenable to exact numerical solution. This is the main objective of the present paper and is accomplished by using the the Lipkin model,<sup>17</sup> commonly employed in nuclear physics to test many-body theories.<sup>18</sup> A special emphasis is put on the calculation of the *fluctuation corrections* by means of the uniform approximation, which are indeed found to be significant, especially in the transition region.

The balance of the paper is as follows. In Sec. II the finite-temperature methods are used to approximate the free energy of the Lipkin model. In Secs. II A and II B we apply the mean-field approximation in the variational approach and in the functional integral approach, respectively. Section II A contains a thermodynamic analog of a theorem of Thouless<sup>19</sup> concerning the stability of the mean-field solutions in a general temperature-dependent Hartree-Fock approximation. The uniform approximation schemes for the inclusion of fluctuations in the mean field are discussed in Secs. II C and II D in the static approximation. In Sec. III the entropy and level density of the Lipkin model are evaluated using the same approximations as in Sec. II. All quantities are compared with their exact values. We find in these model calculations that the uniform approximation provides a significant improvement over the mean-field approximation and that the uniformly approximated thermodynamic functions are in good agreement with their exact values at high excitation energies. Encouraged by these results, we discuss in Sec. IV the potential application of our methods to realistic situations.

## II. LIPKIN MODEL: FREE ENERGY

The Lipkin model<sup>17</sup> is an  $N$  fermion system with two  $N$ -fold degenerate single-particle levels,  $-\epsilon/2$  and  $\epsilon/2$ . If we denote by  $a_{p-1}^\dagger$  ( $p=1, \dots, N$ ) the creation operators for the  $N$  degenerate lower states and by  $a_{p+1}^\dagger$ , those for the higher states, the Lipkin Hamiltonian is the following:

$$\tilde{H} = \frac{1}{2}\epsilon \sum_{p,s=\pm 1} sa_{ps}^\dagger a_{ps} + \frac{1}{2}v \sum_{p,s,s'} a_{ps}^\dagger a_{ps'}^\dagger a_{p-s'} a_{p-s} . \quad (2.1)$$

The first term in the Hamiltonian (2.1) is a one-body operator analogous to a kinetic energy term, while the second represents a two-body interaction characterized by a strength  $v$ . It is possible to define quasispin operators

$$J_\pm = \sum_p a_{p\pm 1}^\dagger a_{p\mp 1} , \quad (2.2)$$

$$J_z = \frac{1}{2} \sum_{ps} sa_{ps}^\dagger a_{ps} ,$$

which close an SU(2) algebra. The Hamiltonian can then be expressed in terms of these operators:

$$\tilde{H} = \epsilon J_z + v(J_x^2 - J_y^2) . \quad (2.3)$$

Since  $[\tilde{H}, \vec{J}^2]=0$ , the Hamiltonian has to be diagonalized within each of the irreducible SU(2) multiplets separately. The ground state multiplet is characterized by  $j=N/2$ , and from now on we shall confine our attention to that multiplet. In the following we shall need to have an interaction which is negative definite. The Hamiltonian (2.3) can be modified to meet this requirement by subtracting from it  $v\vec{J}^2$  (which is a constant for the ground state multiplet):

$$H = \epsilon J_z - v(2J_y^2 + J_z^2) . \quad (2.4)$$

### A. The variational free energy

The exact free energy of a system at temperature  $T=\beta^{-1}$  is found by minimizing the free energy functional

$$F_{\text{var}}[T, D] = \langle H \rangle - TS = \text{Tr} D(T \ln D + H) \quad (2.5)$$

with respect to a normalized trial many-body density matrix  $D$ .

To obtain the temperature-dependent Hartree-Fock approximation we have to minimize (2.5) with respect to densities which are exponentials of one-body operators.<sup>24</sup> Such a trial density matrix for a Lipkin system is

$$D_\lambda = \exp(-\beta \vec{\lambda} \cdot \vec{J}) / \text{Tr} \exp(-\beta \vec{\lambda} \cdot \vec{J}) , \quad (2.6)$$

where  $\vec{\lambda}=(\lambda_x, \lambda_y, \lambda_z)$  are variational parameters. This density is the canonical distribution for a one-body *mean-field* Hamiltonian

$$H_\lambda = \vec{\lambda} \cdot \vec{J} . \quad (2.7)$$

Note, however, that here we consider in the exponent a special type of one-body operator, namely one which can

be expressed as a combination of the quasispin operators (2.2). The restriction to such a type of coherent excitation, which will be applied repeatedly in Sec. II, reduces significantly the number of degrees of freedom and therefore, the amount of calculation. This is a characteristic feature of group theoretic Hamiltonians.

The partition function in the denominator of (2.6) is just the analytic continuation of the character of the corresponding SU(2) representation ( $j=N/2$ ) to imaginary angles:

$$\zeta = \text{Tre}^{-\beta \vec{\lambda} \cdot \vec{J}} = \frac{\sinh[(j + \frac{1}{2})\beta\lambda]}{\sinh\beta\lambda/2}, \quad (2.8)$$

where

$$\lambda = |\vec{\lambda}| = (\lambda_x^2 + \lambda_y^2 + \lambda_z^2)^{1/2}. \quad (2.9)$$

Note that  $\zeta$  is a function only of  $\beta\lambda$ .

In order to calculate (2.5) we need to compute  $\langle J_i \rangle$  and  $\langle J_i J_j \rangle$ . Due to the invariance of the trace under cyclic permutation,  $\langle \vec{J} \rangle$  can be computed from

$$\langle J_i \rangle = -\frac{\partial}{\partial(\beta\lambda_i)} \ln \zeta = -\frac{\zeta'}{\zeta} \frac{\lambda_i}{\lambda}, \quad (2.10)$$

where  $\zeta'$  is the derivative of  $\zeta$  with respect to  $\beta\lambda$ . The group structure of the problem allows us to also compute  $\langle J_i J_j \rangle$  explicitly as shown in Appendix A.

In the mean-field approximation the second variation of  $\beta F$  is not necessarily positive definite, so that  $F$  can have several saddle points. Since for the Hamiltonian (2.4) the free energy  $F_{\text{var}}$  depends on  $\lambda_x$  only through  $\lambda$ ,  $\lambda_x=0$  at all saddle points. Thus, for the purpose of investigating the saddle points of  $F$ , we may consider it as a function of  $\lambda_y$  and  $\lambda_z$  with  $\lambda_x=0$ . Introducing polar coordinates  $\lambda_z = \lambda \cos\phi$ ,  $\lambda_y = \lambda \sin\phi$  and taking  $\epsilon=1$  (so that all energies as well as temperatures are measured in units of  $\epsilon$ ), we have the following:

$$F_{\text{var}} = -\frac{\zeta'}{\zeta} \cos\phi - \kappa v(1 + \sin^2\phi) - \frac{3}{2}v \coth(\beta\lambda/2) \frac{\zeta'}{\zeta} + \lambda \frac{\zeta'}{\zeta} - \beta^{-1} \ln \zeta, \quad (2.11)$$

where

$$\kappa = \frac{\zeta''}{\zeta} - \frac{\zeta'}{2\zeta} \coth(\beta\lambda/2). \quad (2.12)$$

For any given  $\lambda$  the extremal points in  $\phi$  for (2.11) are  $\phi=0$  and the two points

$$\cos\phi = \frac{1}{\chi} \left[ j - \frac{1}{2} \frac{\zeta'/\zeta}{\kappa} \right], \quad (2.13)$$

where we have redefined the coupling parameter  $\chi$  to be  $\chi=(N-1)v$ . The solutions of (2.13) exist only when  $\chi > 1$ . The solution  $\phi=0$  corresponds to the quasispin  $\langle \vec{J} \rangle$  being aligned along the negative axis and will be termed "spherical." The other two solutions ( $\pm\phi \neq 0$ ), when they exist, are degenerate and will be termed "deformed." In the following, we shall assume  $\chi > 1$  (known as the strong coupling region). When the deformed solutions exist, they are minima (in the  $\phi$  direction) and the

spherical one is a maximum. However, as soon as the deformed solutions disappear (for some  $\beta$  and  $\lambda$ ), the spherical solution becomes a minimum. At a given low temperature  $T=\beta^{-1}$  the deformed solutions exist only for  $\lambda$  larger than that determined by the equation

$$(j - \frac{1}{2}) \frac{\zeta'/\zeta}{\kappa} = \chi. \quad (2.14)$$

Note that (2.14) is an equation in  $\beta\lambda \equiv \omega$  and its solution  $\omega_0$  depends only on  $\chi$  and  $N$ .

We find that there is a critical temperature  $\beta_c = \omega_0$  at which a second order "shape" phase transition occurs. Above  $T_c$  the equilibrium configuration is spherical, but as soon as  $T$  decreases below  $T_c$  there is a phase transition to a deformed shape. The deformed minima are characterized by  $\lambda_y \neq 0$  which plays the role of an order parameter. The existence of a shape phase transition in the Lipkin model at finite temperature was already noted in Ref. 21, where coherent states were used to compute the free energy surfaces. However, our approach provides a better variational bound for the free energy.

Contour plots of the free energy (2.11) in the  $\lambda_y$ - $\lambda_z$  plane are shown in Fig. 1 for  $N=50$ ,  $\chi=1.47$ , and for different temperatures. The critical temperature is  $T_c=5.01$ . The free energy  $F$  of the equilibrium configuration is plotted versus  $T$  in Fig. 2. This free energy is compared with the exact free energy calculated from

$$F = -\beta^{-1} \ln \left[ \sum_i e^{-\beta E_i} \right], \quad (2.15)$$

where  $E_i$  are the exact energy levels of the ground state multiplet of the Lipkin Hamiltonian (2.4).

Using the concavity of the entropy it is easy to show that the *exact* function  $\beta F$  is a convex function of  $\beta$ .<sup>22</sup> In Appendix B we demonstrate that in the *mean-field ap-*

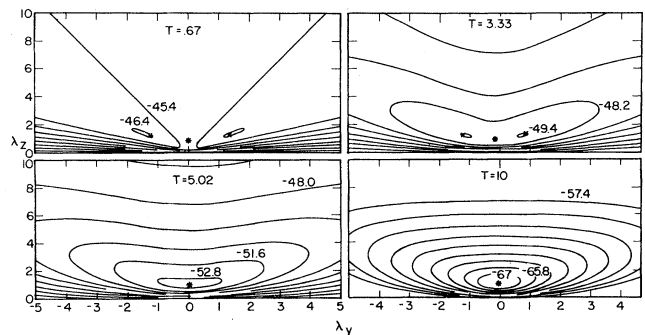


FIG. 1. Contour plots in the  $\lambda_y$ - $\lambda_z$  plane of the variational free energy at different temperatures ( $T=0.67, 3.33, 5.02$ , and  $10$ ) for a Lipkin Hamiltonian (2.4) with  $\chi=1.47$  and  $N=50$ . In this and all following figures, temperatures and free energies are measured in units of  $\epsilon$  (the single-particle level spacing). All contours are spaced 1.2 units apart. The spherical saddle points are marked with asterisks (\*) and the deformed ones with crosses (x). The top two plots are below the critical temperature; the bottom left is at the critical temperature, and the bottom right well above it. Note the broad minimum at the critical temperature.

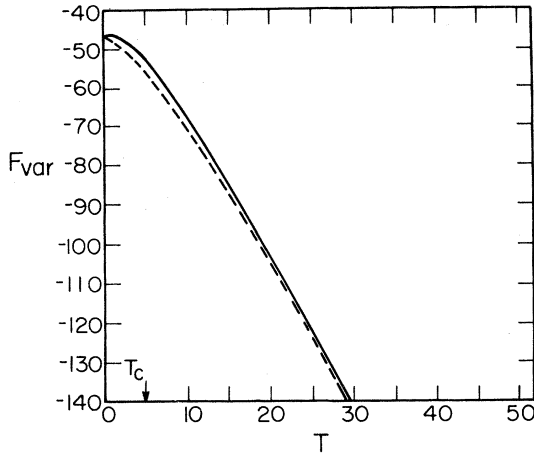


FIG. 2. Variational mean-field free energy (full line) and exact free energy (dashed line) versus temperature  $T$ . Units and parameters are as in Fig. 1. Note that the variational approximation is worst near the critical temperature, which is marked by an arrow.

*proximation* the equilibrium  $\beta F$  is still convex at any point  $\beta$  where there is a stable Hartree-Fock solution.<sup>23</sup> It is common knowledge in thermodynamics that the convexity of  $\beta F$  is a condition for the *thermodynamic* stability of the system. Thus, we have obtained an important result that in the mean-field approximation the thermodynamic stability of the system (with respect to fluctuations in the temperature<sup>24</sup>) follows from the stability of the Hartree-Fock solution on the free energy surface (with respect to fluctuations in the density at constant temperature). The physical content of this result is a thermodynamic analog of a famous theorem of Thouless,<sup>19</sup> who showed that the random phase approximation (RPA) frequencies are all real when the ground-state Hartree-Fock solution is stable on the energy surface. Since the RPA modes are just the normal modes of the TDHF equation linearized around the static HF solution, the reality of the RPA frequencies implies the stability of the system against *dynamical* perturbations. Thus, the content of the Thouless theorem is that the dynamical stability of the system follows from the “static” stability of the Hartree-Fock solution. The reader should note, however, that the proof of the Thouless result is rather different and more complicated due to its dynamical content.

In the limit  $T \rightarrow 0$

$$F/N \rightarrow -\frac{1}{2} \left[ \chi + \frac{1}{2\chi} \right] + O \left[ \frac{1}{N} \right], \quad (2.16)$$

which is just the Hartree-Fock ground state energy.<sup>25</sup> When compared to the exact ground state energy, the error in (2.16) is of order  $1/N$ . The error in the variational free energy becomes even larger around the phase transition since the free energy surface is very flat near  $T_c$  and fluctuations in the mean-field values are important.

## B. The functional integral approach and the static approximation

Since the variational principle is not capable of dealing with fluctuations around the equilibrium configuration, a more sophisticated theory should be applied. Such a theory is based on the functional integral representation of the exact partition function<sup>9</sup> in terms of an infinite number of one body partition functions,

$$Z(\beta) = \frac{\int D[\sigma_y(\tau)] D[\sigma_z(\tau)] e^{-\beta F[\beta, \sigma_y(\tau), \sigma_z(\tau)]}}{\int D[\sigma_y(\tau)] D[\sigma_z(\tau)] e^{-\int_{-\beta/2}^{\beta/2} d\tau [2\sigma_y^2(\tau) + \sigma_z^2(\tau)]}}, \quad (2.17)$$

where

$$F[\beta, \sigma_y(\tau), \sigma_z(\tau)] = \beta^{-1} v \int_{-\beta/2}^{\beta/2} d\tau (2\sigma_y^2 + \sigma_z^2) - \beta^{-1} \ln \text{Tr} (T e^{\int_{-\beta/2}^{\beta/2} d\tau H_\sigma}) \quad (2.18)$$

is the free energy of the one-body Hamiltonian:

$$H_\sigma = J_z - 2v(2\sigma_y J_y + \sigma_z J_z). \quad (2.19)$$

Time dependent mean-field configurations do contribute to the exact partition function but are hard to evaluate. We shall therefore use the static approximation in which only time independent configurations are included in (2.17). It can be shown directly, by completing the squares, that if the noncommutativity of the operators  $J_y$  and  $J_z$  is neglected, then

$$Z(\beta) \simeq \frac{\int d\sigma_y d\sigma_z e^{-\beta F[\beta, \sigma_y, \sigma_z]}}{\int d\sigma_y d\sigma_z e^{-\beta v(2\sigma_y^2 + \sigma_z^2)}}, \quad (2.20)$$

where

$$F[\beta, \sigma_y, \sigma_z] = v(2\sigma_y^2 + \sigma_z^2) - \beta^{-1} \ln \frac{\sinh(j + 1/2)\beta\lambda}{\sinh\beta\lambda/2} \quad (2.21)$$

is the free energy (2.18) in the time-independent mean field  $\sigma_y, \sigma_z$ . Here  $\lambda$  is the magnitude of the vector

$$\vec{\lambda} = (0, -4v\sigma_y, 1 - 2v\sigma_z). \quad (2.22)$$

Note that the integrals in (2.20) are ordinary integrals, so their calculation is significantly simpler than (2.17). The approximation (2.20) is a “classical” approximation since it provides the leading term in a  $1/N$  expansion as shown by scaling the quasispin operators  $j_y = J_y/N$ ,  $j_z = J_z/N$ . Then the Lipkin Hamiltonian undergoes a similar scaling:

$$H/N \simeq j_z - \chi(2j_y^2 + j_z^2). \quad (2.23)$$

Since  $[j_y, j_z] = (i/N)j_x$ , it is clear that any correction to the free energy per particle from time-dependent fluctuations is of order  $1/N$ .

To test the static approximation we have calculated (2.20) by using numerical integration. The results for  $N=50$  and  $\chi=1.47$  are hardly distinguishable from the exact one on the scale of Fig. 2. The ratio of the static

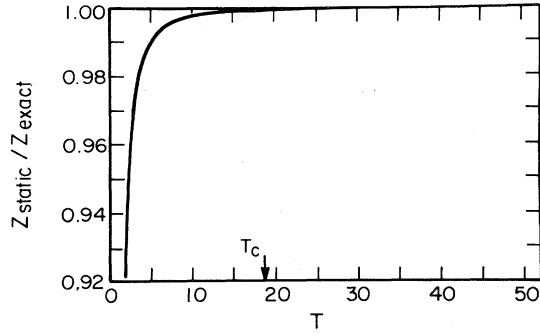


FIG. 3. Ratio of the "static" partition function (2.20) to the exact partition function, versus temperature  $T$  for the Lipkin model. The approximation is better at higher temperatures.

partition function (2.20) to the exact one is plotted in Fig. 3. We see that the static approximation becomes better for higher temperatures. Indeed, as the "time" interval  $\beta$  in (2.18) becomes shorter, we expect the time dependent fluctuations to be less important. However, even at temperatures down to  $T \sim 2$ , the error for  $N = 50$  is only about 10%. This difference should be accounted for by the RPA corrections at finite temperature.<sup>9,20</sup>

### C. The mean field approximation

In a realistic problem, the integral in (2.20) is still infinite dimensional and has to be evaluated by some approximation method. The simplest one is the saddle point method, where one assumes that the main contribution to the integral comes from the points where  $F$  in (2.21) has a minimum. Thus, as in the variational approach, we have to investigate the topology of the free energy surface at different temperatures. As noted in Appendix A of Ref. 13, although the free energy surface in the functional integral differs from the variational one, they both have the same topology of saddle points. Indeed, we see this in Fig. 4, where the functional integral free energy (2.21) is shown at different temperatures.

The spherical saddle point is now given by  $\sigma_y^0 = 0$  and  $\sigma_z = \sigma_z^0$  which is found from the solution of  $\sigma_z = -\xi'/\xi$ ,

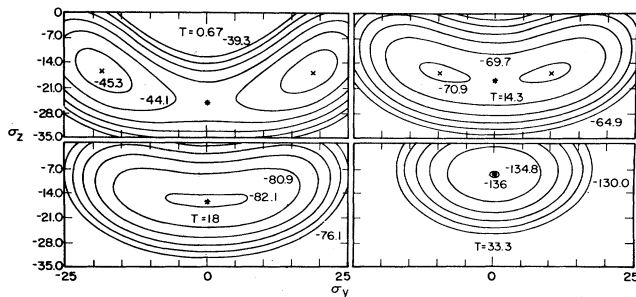


FIG. 4. As in Fig. 1, but for the "functional integral" free energy (2.18) and at temperatures  $T = 0.67, 14.3, 18$  (critical temperature), and  $33.3$ .

where  $\lambda = |1 - 2v\sigma_z|$ . The degenerate deformed solutions which exist below a certain critical temperature  $T_c$  are characterized by  $\sigma_z^1 = \sigma_z^2 = -1/(2v)$  and by  $\sigma_y^1 = -\sigma_y^2$  which solve

$$\frac{\lambda}{4v} = -\xi'/\xi, \quad (2.24a)$$

where

$$\lambda = 2(1 + 4v^2\sigma_y^2)^{1/2}. \quad (2.24b)$$

At  $T = T_c$  the three solutions coalesce and there is a single minimum at  $\sigma_y = 0, \sigma_z = -1/(2v)$ . Since  $\sigma_y$  becomes nonzero as  $T$  decreases from  $T_c$  it may be identified as an order parameter. The transition occurs when the solution to (2.24) is  $\sigma_y = 0$ , so that  $T_c$  is determined from

$$\left. \frac{\xi'}{\xi} \right|_{2\beta_c} = \frac{1}{2v}. \quad (2.25)$$

The mean-field free energy, which is the global minimum of  $F$  in (2.21), is plotted against  $T$  in Fig. 5 (dotted-dashed line), where the deformed value is used below  $T_c$  and the spherical one above  $T_c$ .

It is important to note that contrary to the general case (see Ref. 13), the above mean-field free energy does *not* coincide with the variational one (shown in Fig. 2) and the critical temperatures differ as well. The reason for this apparent contradiction is that here we are restricting ourselves to coherent configurations only in both the functional integral (2.17) and the variational trial state (2.6). However, the difference in the above two free energies per particle is only of order  $1/N$ . For instance, in the limit  $T \rightarrow 0$  we find from (2.21)

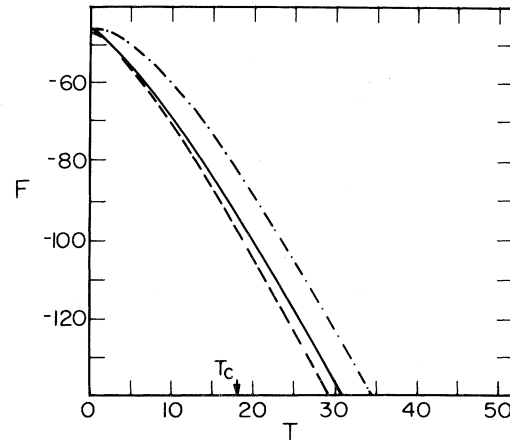


FIG. 5. Approximate and exact free energies  $F$  of the Lipkin model versus temperature  $T$ . The dotted-dashed line is the mean-field free energy [calculated at the equilibrium configuration of (2.21)]. The full line includes the fluctuations in the order parameter  $\sigma_y$  alone [calculated in the uniform approximation (2.32) and (2.41)]. The dotted line is the free energy obtained when fluctuations in both  $\sigma_y$  and  $\sigma_z$  are accounted for [(2.32) and (2.33)], but is indistinguishable on this scale from the exact free energy (dashed line).

$$F \rightarrow -j \left[ \chi + \frac{1}{2\chi} \right] + \frac{1}{2\chi} - \frac{j}{2j-1} \chi, \quad (2.26)$$

which differs from the variational result (2.16), when calculated per particle, by  $O(1/N)$ .

When  $T \sim T_c$ , the two deformed saddle points are too close to each other and the approximation breaks down. Indeed, the mean-field approximation is worst around  $T_c$  as can be seen from Fig. 6, where the fractional error of the approximation is plotted versus  $T$ . In the next subsection, we shall show how to modify the approximation in that region.

#### D. Inclusion of fluctuations: The uniform approximation

A generalization of the saddle point method is known in the literature as the uniform approximation.<sup>15,16</sup> This approximation is valid in the transition region where the saddle points coalesce, as well as far from it where it reduces to the saddle point approximation. Since the uniform method yields a universal analytic expression for the partition function<sup>13</sup> (for a given topology of saddle points), it is instructive to apply it in our case.

At any given temperature, we define a mapping  $\sigma_y, \sigma_z \rightarrow u, z$  which will map  $\beta F$  onto a simpler analytic function with the same saddle point topology:

$$\beta F[\beta, \sigma_y, \sigma_z] = g(u) + \xi_0 + \frac{1}{2}z^2. \quad (2.27)$$

The simplest choice for  $g$  in our case is

$$g(u) = \frac{1}{4}u^4 - \frac{1}{2}\xi_1 u^2. \quad (2.28)$$

Here,  $\xi_0, \xi_1$  are constants (which depend on  $T$ ) and are known as the control parameters. When  $\xi_1 > 0$ , the right-hand side of (2.27) has one saddle point and two degenerate minima, while when  $\xi_1 < 0$  it has a unique *real* minimum. This is identical to the saddle-point topology of  $F$ . Note that there is no linear term in  $u$  since the two deformed saddle points are always degenerate and that at the transition temperature  $\xi_1 = 0$ . The constants  $\xi_0, \xi_1$  are determined by the conditions that the saddle points of  $F$  be mapped onto those of  $g$ :

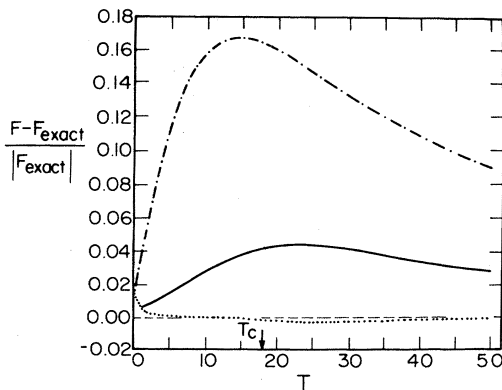


FIG. 6. As in Fig. 5, but for the fractional error in the approximate free energies  $(F - F_{\text{exact}}) / |F_{\text{exact}}|$ .

$$\beta F[\beta, \sigma_y^0, \sigma_z^0] = \xi_0, \quad (2.29a)$$

$$\beta F[\beta, \sigma_y^1, \sigma_z^1] = -\frac{1}{4}\xi_1^2 + \xi_0. \quad (2.29b)$$

Here  $(\sigma_y^0, \sigma_z^0)$  is the spherical saddle point and  $(\sigma_y^1, \sigma_z^1)$  is one of the two deformed points. To evaluate the numerator integral in (2.20), we first transform the integration variables to  $(u, z)$ :

$$\int d\sigma_y d\sigma_z e^{-\beta F[\beta, \sigma_y, \sigma_z]} = \int du dz J(u, z) e^{-g(u) - \xi_0 - (1/2)z^2}, \quad (2.30)$$

where

$$J(u, z) = \partial(\sigma_y, \sigma_z) / \partial(u, z)$$

is the Jacobian of the mapping. The next step is to expand  $J$  in terms of a quantity which vanishes simultaneously at all of the saddle points, e.g.,  $u(u^2 - \xi_1)$ :

$$J(u, z) = \sum_{m, n} \{ a_{mn} [u(u^2 - \xi_1)]^{mz^n} + b_{mn} u [u(u^2 - \xi_1)]^{mz^n} + c_{mn} u^2 [u(u^2 - \xi_1)]^{mz^n} \}, \quad (2.31)$$

where  $a_{mn}$ ,  $b_{mn}$ , and  $c_{mn}$  are the expansion coefficients. The coefficients  $a_{00}$ ,  $b_{00}$ , and  $c_{00}$  (which we shall denote by  $a_0$ ,  $b_0$ , and  $c_0$ , respectively) are found from the values of the Jacobian at the three saddle points. The uniform approximation is obtained from (2.30) by keeping only the  $m = n = 0$  terms in expansion (2.31). The partition function in (2.20) is then approximated by

$$Z(\beta) = 2e^{-\beta F_0} [\tilde{a}_0 I_0(\xi_1, 0) + \tilde{c}_0 I_2(\xi_1, 0)], \quad (2.32)$$

where

$$\tilde{a}_0 = \left[ \frac{2}{\pi} \right]^{1/2} \beta v a_0 = \left[ \frac{2}{\pi} \right]^{1/2} v \left[ \frac{\xi_1}{-\det F_0''} \right]^{1/2} \quad (2.33a)$$

and

$$\tilde{c}_0 = 2 \left[ \frac{2}{\pi} \right]^{1/2} \beta v c_0 = 2 \left[ \frac{2}{\pi} \right]^{1/2} \frac{v}{\xi_1} \left[ \frac{2\xi_1}{\det F_1''} \right]^{1/2} - \left[ \frac{\xi_1}{-\det F_0''} \right]^{1/2}. \quad (2.33b)$$

In (2.32),  $I_n(\xi_1, 0)$  are universal analytic functions defined by

$$I_n(\xi_1, 0) = \int_{-\infty}^{\infty} du u^n e^{-u^4 + \xi_1 u^2}. \quad (2.34)$$

The universal functions  $I_n$  of two arguments were introduced in Ref. 13. Here we have a special case in which the second argument is zero. A nonzero second argument characterizes a *first order* phase transition which can occur when the two deformed minima are not degenerate. The function  $I_0(\xi_1, 0)$  can be expressed in terms of the *parabolic cylinder* functions  $U$  and  $V$  or in terms of Bessel

functions of fractional order which are more useful for numerical calculations.<sup>26</sup>

At a given temperature, all of the parameters which occur in (2.32), namely  $\xi_0$ ,  $\xi_1$ ,  $\tilde{a}_0$ , and  $\tilde{c}_0$ , are completely determined from  $F_0, F_1$  and  $\det(F_0''), \det(F_1'')$  by (2.29) and (2.33). Note that these equations also hold above the critical temperature ( $T > T_c$ ). In that case, the only *real* saddle point is the spherical one ( $\sigma_y^0, \sigma_z^0$ ) and the two deformed saddle points become *complex*. Although these saddle points are not physical, they still have to be taken into account in (2.29) in order to determine the mapping. Especially just above  $T_c$  these points are close to the spherical one and, therefore, affect the saddle-point approximation. For these points, we still have  $\sigma_z = -1/(2v)$ , but the  $\sigma_y$  which satisfies (2.24) is *purely imaginary*. As  $T$  continues to increase,  $\lambda$  becomes purely imaginary, too. In this case, since  $\xi$  is a periodic function on the imaginary axis, (2.24a) has many imaginary solu-

tions for  $\lambda$ , among which we choose the one *closest* to the real axis. Figure 7 shows the temperature dependence of the control parameter  $\xi_1$  and of the "normalized" expansion parameters  $\tilde{a}_0$  and  $\tilde{c}_0$  (continuous lines) for the Lipkin model with  $N=50$  and  $\chi=1.47$ . The uniform free energy calculated from the partition function (2.32) is in very close agreement with the exact one, as Figure 6 shows.

When  $T \ll T_c$  or  $T \gg T_c$  the saddle points are well separated and the uniform approximation should reduce to the ordinary saddle point results.

(i)  $T \ll T_c$

In this case  $\xi_1$  is positive and large. We can then use the asymptotic expansion of  $V$  [see (19.8.2) in Ref. 26] to find

$$Z(\beta) \sim 2 \frac{2^{5/4} v}{\sqrt{\det F_1''}} e^{-\beta F_1}. \quad (2.35)$$

The result (2.35) is exactly what we obtain if we evaluate (2.20) by the saddle point method. (For  $T \ll T_c$  only the two deformed saddle points contribute and their contributions are equal.) In the limit  $T \rightarrow 0$  we have from (2.35)

$$\beta F \simeq (\beta F_1 - \ln 2) - \frac{1}{2} \ln[\sqrt{2}\chi^2/(\chi^2 - 1)], \quad (2.36)$$

where  $F_1$  is given by (2.26). Note that  $(\beta F_1 - \ln 2)$  is the approximation for  $\beta F$  when fluctuations are neglected (taking into account the degeneracy of the two deformed points). We see from (2.36) that the fluctuation corrections for  $\beta F$  in the limit  $T \rightarrow 0$  are finite and negative.

(ii)  $T \gg T_c$

Here  $\xi_1$  is negative and large in magnitude. Using (19.8.1), of Ref. 26, and neglecting the  $c_0$  term we find

$$Z(\beta) \sim \frac{2^{3/2} v}{\sqrt{\det F_0''}} e^{-\beta F_0}, \quad (2.37)$$

which is again just the saddle point approximation of (2.20). Indeed, for  $T \gg T_c$  there is a single real saddle point (the spherical minimum).

#### E. Inclusion of fluctuations in the order parameter only

For a general many-body system, the determinants in (2.33) are still infinite dimensional. A more practical, but cruder, approximation is one in which only fluctuations in certain constrained directions which play the role of order parameters are taken into account. For instance, these directions were chosen in Ref. 13 to be the quadrupole deformations of the nucleus. In the present model, the order parameter is  $\sigma_y$ , and we can compute the free energy "surface":

$$\tilde{F}[\beta, \sigma_y] = \min_{\sigma_z} F[\beta \sigma_y, \sigma_z] \Big|_{\sigma_y = \text{const}}. \quad (2.38)$$

The free energy of (2.38) is plotted versus  $\sigma_y$  in Fig. 8, for the same temperatures as in Fig. 4. Indeed, it exhibits most of the features of the phase transition seen in the more detailed picture of Fig. 4. For instance, the saddle points are the same in both pictures. As for the fluctuations, we hope that those in all "other" directions ( $\sigma_z$  in our case) would to a large extent be canceled in the numerator and denominator of (2.20) and that the approx-

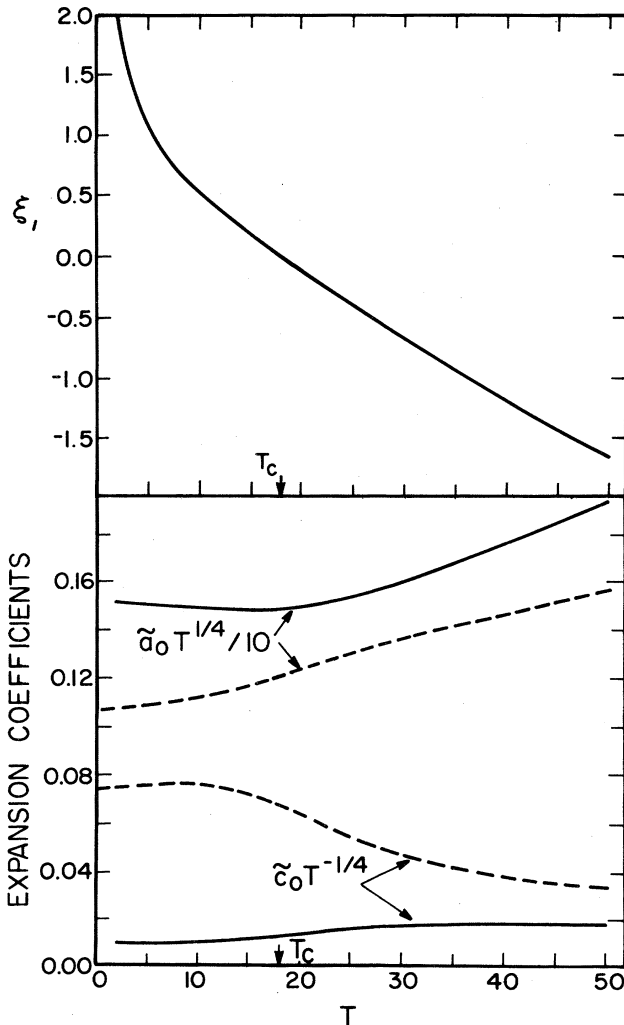


FIG. 7. The temperature dependence of parameters in the uniform approximation [see (2.32)] for the Lipkin model. Top: Control parameter  $\xi_1$  vs temperature  $T$ . Bottom: "Normalized" expansion coefficients  $\tilde{a}_0$  and  $\tilde{c}_0$  vs temperature  $T$  as calculated from (2.33) (dashed lines) and (2.41) (solid lines). The coefficients have been scaled by  $T^{\pm 1/4}$  as shown in the figure.

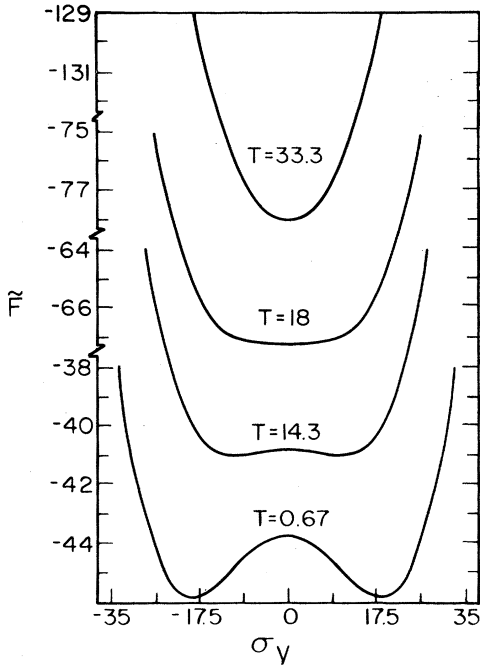


FIG. 8. Free energy  $\tilde{F}$  [see (2.38)] of the Lipkin model versus the order parameter  $\sigma_y$ , at different temperatures (those of Fig. 5). These curves are used to calculate the free energy represented by the full lines in Fig. 5.

imation be based on fluctuations in the important directions only:

$$Z(\beta) \simeq \frac{\int d\sigma_y e^{-\beta\tilde{F}[\beta, \sigma_y]}}{\int d\sigma_y e^{-2\beta v \sigma_y^2}} \quad (2.39)$$

will be reasonable. The normalization integral in the denominator of (2.39) is obtained from that in (2.20) by minimizing the "action" in the  $\sigma_z$  direction (i.e., setting  $\sigma_z=0$ ). This is the same approximation as is used in the numerator. We note that this normalization integral is also temperature dependent.

Equation (2.39) can also be evaluated by the uniform approximation. The mapping is a one-variable mapping ( $\sigma_y \rightarrow u$ ) such that:

$$\beta\tilde{F}[\beta, \sigma_y] = \frac{1}{4}u^4 - \frac{1}{2}\xi_1 u^2 + \xi_0. \quad (2.40)$$

The final result for the approximated partition function is in the form (2.32). The numerical control parameter  $\xi_1$  is exactly the same as that of Sec. IID. The only difference arises in the coefficients  $\tilde{a}_0, \tilde{c}_0$  which are now given by

$$\tilde{a}_0 = \left(\frac{\beta v}{\pi}\right)^{1/2} a_0 = \left(\frac{v}{\pi}\right)^{1/2} \left[\frac{\xi_1}{\tilde{F}_0''}\right]^{1/2}, \quad (2.41a)$$

$$\tilde{c}_0 = 2 \left(\frac{\beta v}{\pi}\right)^{1/2} c_0 = \left(\frac{v}{\pi}\right)^{1/2} \frac{2}{\xi_1} \left[\frac{2\xi_1}{\tilde{F}_1''}\right]^{1/2} - \left[\frac{\xi_1}{-\tilde{F}_0''}\right]^{1/2}. \quad (2.41b)$$

Here  $\tilde{F}_0''$  and  $\tilde{F}_1''$  refer to ordinary second derivatives of  $\tilde{F}$  (with respect to  $\sigma_y$  at the spherical and deformed configurations, respectively). The expressions (2.33a) and (2.33b) for  $\tilde{a}_0$  and  $\tilde{c}_0$  in Sec. IID differ from (2.41a) and (2.41b) also by an additional  $\sqrt{2v}$  normalization factor. This is related to the presence of a second direction for fluctuations in the former calculation. Indeed, in the limit  $N=0(j=0)$  we have  $F=2v\sigma_y^2+v\sigma_z^2$ ,  $\tilde{F}=2v\sigma_y^2$ , and thus  $\det F_0''$  contains an additional factor of  $2v$  as compared with  $\tilde{F}_0''$ .

The coefficients  $\tilde{a}_0$  and  $\tilde{c}_0$  calculated from (2.41) are plotted in Fig. 7 (dashed lines) and are of the same order of magnitude as the ones calculated from (2.33). The free energy calculated from (2.32) and (2.41) is shown by the continuous line in Fig. 5. We can see that the inclusion of fluctuations in the order parameter alone already provides a significant improvement over the mean-field free energy and accounts for much of the difference between the mean-field and exact free energies (see also Fig. 6).

The transition approximation, a power series expansion of the free energy about the spherical solution<sup>27</sup> valid for  $T \sim T_c$ , can be derived for the one-dimensional case, where we can expand the free energy  $\tilde{F}$  to sixth order around the spherical solution. The final results for  $a_0$  and  $c_0$  in terms of the derivatives of  $\tilde{F}$  at the critical point are the following:

$$a_0(T_c) = \left[\frac{6}{\tilde{F}^{(iv)}}\right]^{1/2}, \quad (2.42a)$$

$$c_0(T_c) = -\frac{6^{3/4}}{40} \frac{\tilde{F}^{(vs)}}{[\tilde{F}^{(iv)}]^{7/4}}. \quad (2.42b)$$

### III. LIPKIN MODEL: ENTROPY AND LEVEL DENSITY

#### A. Entropy

We must first find the entropy as a function of temperature by using

$$S = -\partial F / \partial T, \quad (3.1)$$

and then calculate the energy from  $E = F + TS$ . In Fig. 9 we plot the entropy versus the energy, which is also considered to be a fundamental relation in thermodynamics. The critical energies at which the phase transitions occur are shown by arrows. We see that the mean-field entropy (dotted-dashed line) lies below the exact entropy (dashed line) for all energies, but that the inclusion of the fluctuations in the order parameter (continuous line) improves the mean-field results substantially. When the (static) fluctuations in the other directions are taken into account as well (dotted line), the agreement with the exact entropy is very good, except near the ground-state energy.

Since all of the energy curves are monotonically increasing with temperature, it follows that  $\partial^2(\beta F) / \partial \beta^2 > 0$  everywhere, and therefore that all of our approximations produce free energies which are *thermodynamically stable*. Note that the maximal energy attainable by the "exact"



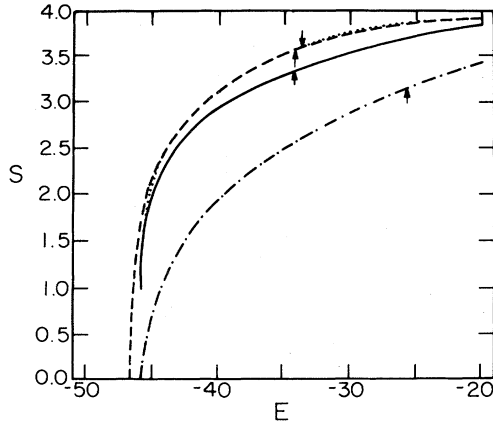


FIG. 9. Approximate and exact entropies  $S$  as a function of energy  $E$ . The various curves are essentially the Laplace transforms of the corresponding curves in Fig. 5. The monotonicity of the different curves indicates that all of our approximations are *thermodynamically stable*. Arrows indicate critical energies which correspond to the critical temperature in the various approximations.

curve is the center of gravity of the Lipkin spectrum. To reach higher energies we have to introduce *negative* temperatures. Also note that the critical energies, which correspond to the critical temperature  $T_c$ , are different in the various approximations.

To calculate the entropy in the mean-field approximation, note that, since

$$\partial F / \partial \sigma_y = \partial F / \partial \sigma_z = 0$$

at the equilibrium configuration, it is enough to take in (2.21) a partial derivative with respect to  $T$  at *constant*  $\sigma_y$  and  $\sigma_z$ . We find for the entropy

$$S_{\text{MF}}(T) = \ln \xi - \beta \lambda \xi' / \xi \quad (3.2)$$

and for the energy

$$E = v(2\sigma_y^2 + \sigma_z^2) - \lambda \xi' / \xi. \quad (3.3)$$

Here  $\xi$  and  $\lambda$  are as in (2.8) and (2.22), and  $\sigma_y$  and  $\sigma_z$  are taken to be at their equilibrium values. Since the transition is of second order, the mean-field entropy and energy are continuous at the transition, but their derivatives are not. When  $T \rightarrow 0$ ,  $\xi' / \xi \rightarrow j$  and from (3.2) we find  $S_{\text{MF}} \rightarrow 0$ , as does the exact entropy. The mean-field energy at this limit is given by (2.26). At the opposite limit,  $T \rightarrow \infty$ , the mean-field entropy approaches  $\ln(N+1)$ , i.e., the logarithm of the number of states, as for the exact entropy.

To find the fluctuation corrections to the entropy we have to use the uniform expression (2.32) in (3.1). The resulting expression is quite complicated and instead we have calculated the derivative numerically. Simpler expressions can be obtained in the limits  $T \ll T_c$  or  $T \gg T_c$  by using the saddle point formulas. For example, when  $T \rightarrow 0$ , we find from (2.35)

$$S(T=0) \simeq \ln[2^{9/4} \chi^2 / (\chi^2 - 1)]. \quad (3.4)$$

This entropy is finite ( $\simeq 1.16$  for  $N=50$  and  $\chi=1.47$ ), as opposed to the exact one which vanishes at  $T=0$ . Indeed, as already discussed in Sec. II B, the approximation employing only time-independent fluctuations is not expected to be good at very low temperatures. However, as soon as  $T \geq 1$  the above approximation is valid. The static fluctuation corrections have no effect on the energy at  $T=0$  (2.36), which is still equal to the mean-field result (2.26).

### B. Level density

The many-body level density  $\rho(E)$  is given from (1.1) as the inverse Laplace transform of the partition function  $Z(\beta)$ . There exist exact numerical methods for the inversion of Laplace transforms which use only real values,<sup>28</sup> but here we shall consider only the saddle point approximation, which yields the standard expression for an average level density<sup>29</sup>

$$\rho(E) \simeq \frac{1}{2\sqrt{\pi\Delta}} e^{S(E)}, \quad (3.5)$$

where  $\Delta^2 = -\partial E / \partial \beta$  is the energy variance in the corresponding canonical distribution. Note that due to their thermodynamic stability (see Sec. III A) all of our approximations satisfy  $-\partial E / \partial \beta > 0$ , so that  $\Delta$  above is always *real*. Note also, however, that when  $T \rightarrow 0$ ,  $\Delta \rightarrow 0$  and approximation (3.5) breaks down.

In the mean-field limit, analytic expressions are easily obtained from (3.3). At  $T=T_c$  there is a discontinuity given by

$$\left[ \left[ -\frac{\partial E}{\partial \beta} \right]_+ - \left[ -\frac{\partial E}{\partial \beta} \right]_- \right]_{T=T_c} = \frac{v}{2T_c}. \quad (3.6)$$

The uniform expressions are more complicated and thus we have chosen to calculate the derivative numerically. The various level density curves are plotted in Fig. 10 versus energy. We see that the mean-field approximation underestimates the exact level density (i.e., the one obtained from the exact free energy) by a factor of  $\sim 2$ . When fluctuations in  $\sigma_y$  only are included, we get about 70% of the exact level density, and most of the rest is accounted for by fluctuations in the  $\sigma_z$  direction. Note that these level densities diverge at the ground state energy. It is easy to show that the mean-field density diverges like  $T^{-1/2}$ , so that its integral (which gives the number of states) is still finite. The "jump" in the mean-field level density which is seen in Fig. 10 is a result of the discontinuity (3.6). No such discontinuities are observed in the uniform curves as they are smoothed out by the fluctuations. It is important to keep in mind that the level density which we are referring to is an *average* level density. The *exact* level density is, of course, a highly singular function

$$\rho(E) = \sum_i \delta(E - E_i), \quad (3.7)$$

where  $E_i$  are the energy levels of the many-body system. Experimental level densities, however, are usually aver-

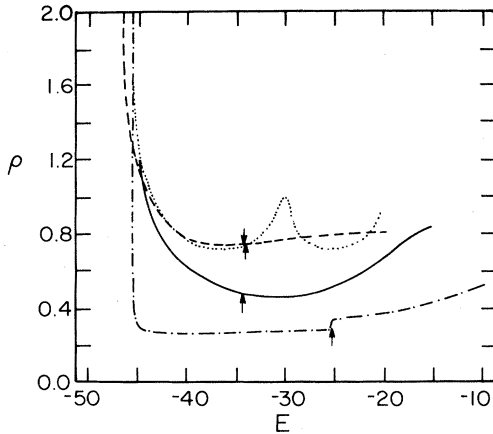


FIG. 10. Level densities  $\rho$  in the Lipkin model versus energy  $E$ . The various level densities were calculated from (3.5) by using the corresponding curves of Figs. 5 and 9. Energy is measured in units of  $\epsilon$  and  $\rho$  in units of  $\epsilon^{-1}$ . Arrows are as in Fig. 9.

aged over a certain width. To obtain such an average level density from (3.7), we have applied a Strutinsky-type smoothing<sup>30</sup>

$$\bar{\rho}(E) = \frac{1}{\gamma} \sum_i f \left( \frac{E - E_i}{\gamma} \right), \quad (3.8)$$

where the smoothing function  $f$  is

$$f(x) = L_M^{1/2}(x^2) e^{-x^2}. \quad (3.9)$$

Here  $L_M^{1/2}$  is a generalized Laguerre polynomial.<sup>26</sup> The energy interval  $\gamma$  and the order  $M$  of the polynomial are chosen such that  $\bar{\rho}(E)$  in (3.8) will be insensitive to changes in  $\gamma$  and  $M$ . The average level density compares quite well with the one derived from (3.5) using the exact entropy, as seen in Fig. 11. Significant deviations are ob-

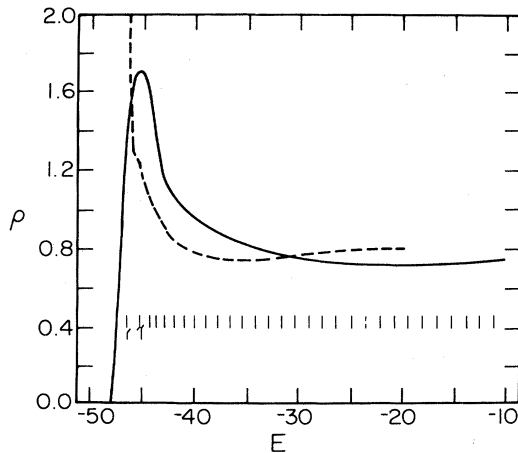


FIG. 11. The dashed line level density of Fig. 10 [obtained when the exact free energy is used in (3.5)] compared with an average level density (full line). This average level density is obtained from the exact level density with a Strutinsky-type smoothing (3.8) and (3.9) with  $\gamma \approx 1.75$  and  $M = 3$ .

served only near the ground state energy where the classical approximation (3.5) breaks down. This figure also includes the spectrum of the present system. We see that near the ground state energy, where states appear in almost degenerate doublets, the average level density is about 2. However, this density drops quickly to an almost constant density of about 1, as the states become nearly evenly spaced (note that the average distance between levels is  $\sim \epsilon = 1$ ). Since the level density (3.5) diverges at the ground state energy, its drop has to be steeper than that of  $\bar{\rho}$  so as to provide the same number of states below a given energy. Note that the average level density (3.8) is symmetric around the mean energy  $(\sum_i E_i)/(N+1)$  of the Lipkin spectrum. Therefore, it is enough to estimate the level density below this point, and we can avoid the introduction of negative temperatures.

#### IV. SUMMARY AND DISCUSSION

In this paper, we have investigated the validity of various approximations for the nuclear partition function and for the many-body level density in the context of an exactly solvable many-body system—the Lipkin model. We conclude that, since the nucleus has a finite number of particles, density fluctuations around the mean-field equilibrium configuration can contribute significantly to the nuclear partition function. These fluctuations are important especially in the vicinity of a phase transition between two different types of nuclear shapes. Generally the fluctuation corrections lower the free energy and increase the level density calculated in the mean-field approximation. Another effect of the fluctuation corrections is to smooth out various singularities of the thermodynamic functions which exist in the mean-field theory at the transition point.

Since the inclusion of time-dependent fluctuations involves the difficult problem of solving the *finite-temperature* RPA equations,<sup>9,20</sup> we have investigated the more practical approximation in which only static fluctuations are considered and found it to be very good for temperatures which are not too low. However, in realistic situations, even this approximation is quite impractical, and instead we use an approximation in which only time-independent fluctuations along certain *constrained directions* are taken into account.

We conclude, from our model calculations, that when the important constraints have been identified, the latter approximation can account for a significant fraction of the difference between the averaged exact level density and the mean-field density. This approximation requires only the knowledge of the free energy surfaces for the constrained variables at different temperatures. While calculations of these surfaces for realistic nuclei by the constrained Hartree-Fock method may still be hard,<sup>12</sup> they are certainly *possible* by the Strutinsky method generalized to finite temperature.<sup>10,11</sup> It would be interesting to carry out such calculations since we can then use the above approximation to evaluate fluctuation corrections<sup>13</sup> to nuclear level densities, previously calculated using realistic independent particle schemes.<sup>14</sup>

Another important direction which we are currently following is the application of the methods developed in

this work to more complicated but *realistic* group Hamiltonians. The advantage of such Hamiltonians is that major simplifications occur in the application of our approximation methods. Most important, the number of relevant degrees of freedom is reduced considerably. For instance, when only static fluctuations are considered, the number of fluctuating variables is always *finite*, and the functional integrals reduce the ordinary integrals. Also, several quantities, such as the free energy surface, can be evaluated analytically by using group theoretical methods. Although the numerical diagonalization of such group Hamiltonians can become extremely hard, if not impossible, when the corresponding representation of the group includes a very large number of states, our approximation schemes remain *tractable*. Such a situation occurs, for example, in polyatomic molecules which can be described by coupled SU(4) groups.<sup>31</sup> In these cases, our methods can be used to evaluate the level density at high excitation energies.

#### ACKNOWLEDGMENTS

One of us (Y.A.) would like to thank S. Levit and R. Balian for many useful discussions during the early stages of this work. We are both grateful to F. Iachello for valuable discussions and to D. A. Bromley for his comments and critical review of our manuscript. This work was supported in part by the U. S. Department of Energy under Contract No. DE-AC02-76ER03074.

#### APPENDIX A: COMPUTATION OF $\langle J_i J_j \rangle$

We rewrite (2.10) as

$$\text{Tr}(J_i e^{-\beta \vec{\lambda} \cdot \vec{J}}) = -\xi' \frac{\lambda_i}{\lambda}, \quad (\text{A1})$$

and take a derivative with respect to  $\beta \lambda_j$  to find

$$\text{Tr}(J_i L_j e^{-\beta \vec{\lambda} \cdot \vec{J}}) = \left[ \xi'' - \frac{\xi'}{\lambda \beta} \right] \frac{\lambda_i \lambda_j}{\lambda^2} + \frac{\xi'}{\lambda \beta} \delta_{ij}, \quad (\text{A2})$$

where

$$\begin{aligned} L_j &= -\frac{\partial}{\partial(\beta \lambda_j)} e^{-\beta \vec{\lambda} \cdot \vec{J}} \\ &= \left[ (\lambda - \beta^{-1} \sinh \lambda \beta) (\vec{\lambda} \cdot \vec{J}) \vec{\lambda} \right. \\ &\quad \left. + \frac{\sinh \lambda \beta}{\lambda \beta} \vec{J} + 2i \frac{\sinh(\lambda \beta / 2)}{\lambda^2 \beta} \vec{\lambda} \times \vec{J} \right]_j. \end{aligned} \quad (\text{A3})$$

The last equality in (A3) is a group property and can be easily proved by using the spin- $\frac{1}{2}$  representation of SU(2). Relation (A3) can be inverted to give

$$\begin{aligned} \vec{J} &= \frac{\lambda \beta}{2} \coth \frac{\lambda \beta}{2} \vec{L} + \frac{1}{\lambda^2} \left[ 1 - \frac{\lambda \beta}{2} \coth \frac{\lambda \beta}{2} \right] (\vec{\lambda} \cdot \vec{L}) \vec{L} \\ &\quad - \frac{i}{2} \beta \vec{\lambda} \times \vec{L}. \end{aligned} \quad (\text{A4})$$

Using (A2) and (A4) we obtain

$$\frac{1}{2} (\langle J_i J_j \rangle + \langle J_j J_i \rangle) = \kappa \frac{\lambda_i \lambda_j}{\lambda^2} + \coth \frac{\lambda \beta}{2} \frac{\xi'}{2 \xi} \delta_{ij}, \quad (\text{A5})$$

where  $\kappa$  is given by (2.12).

#### APPENDIX B: THERMODYNAMIC STABILITY IN THE MEAN-FIELD APPROXIMATION

We shall denote by  $\rho$  the single-particle density matrix corresponding to a  $D$  which is an exponential of a one-body matrix. We show that if, for a given  $\beta$  the mean-field solution  $\rho$  is stable, i.e.,  $\delta_p^2(\beta F[\beta, \rho]) > 0$ , then the thermodynamic function  $\beta F(\beta) = \min_{\rho} F[\beta, \rho]$  is convex at that point, i.e.,

$$\delta^2[\beta F(\beta)] < 0. \quad (\text{B1})$$

Note that under general and independent variations of  $D$  and  $\beta$  in (2.5) we have the following:

$$\delta(\beta F_{\text{var}}[\beta, D]) = \text{Tr} \delta D (\ln D + \beta H) + \delta \beta \langle H \rangle \quad (\text{B2})$$

and

$$\begin{aligned} \delta^2(\beta F_{\text{var}}[\beta, D]) &= \text{Tr}(\delta D \delta \ln D) + \text{Tr} \delta^2 D (\ln D + \beta H) \\ &\quad + 2 \delta \beta \delta \langle H \rangle. \end{aligned} \quad (\text{B3})$$

However, along the mean-field solution  $\rho$ , the first term on the right-hand side of (B2) vanishes so that

$$\delta[\beta F(\beta)] = \delta \beta \langle H \rangle. \quad (\text{B4})$$

Taking directly the variation of (B4) we have

$$\delta^2[\beta F(\beta)] = \delta \beta \delta \langle H \rangle. \quad (\text{B5})$$

An alternative expression for  $\delta^2[\beta F(\beta)]$  is obtained from (B3) where  $D$  is taken to be the mean-field solution at  $\beta$  and  $D + \delta D$  the one at  $\beta + \delta \beta$ . Comparing this expression with (B5) we find

$$\delta^2[\beta F(\beta)] = -\text{Tr}(\delta D \delta \ln D) - \text{Tr} \delta^2 D (\ln D + \beta H). \quad (\text{B6})$$

On the other hand, the right-hand side of (B6) is just  $-\delta_p^2(\beta F[\beta, \rho])$  in which the second variation is with respect to a  $\delta \rho$  along the mean-field solution. Since the Hartree-Fock solution is assumed to be *stable*, (B1) follows immediately.

<sup>1</sup>See, for example, in W. U. Schröder, J. R. Birkelund, J. R. Huizenga, K. L. Wolf, and V. E. Viola, Phys. Rep. **45**, 301 (1978); M. Lefort and C. Ngô, Ann. Phys. (N.Y.) **3**, 5 (1978); A. Gobbi and W. Nörenberg, in *Heavy Ion Collisions*, edited by R. Bock (North-Holland, New York, 1980), Vol. 2, pp.

128–273.

<sup>2</sup>See, for example, in V. V. Volkov, Phys. Rep. **44**, 93 (1978); Y. Alhassid, R. D. Levine, J. S. Karp, and S. G. Steadman, Phys. Rev. C **20**, 1789 (1979).

<sup>3</sup>H. B. Callen, *Thermodynamics* (Wiley, New York, 1960).

- <sup>4</sup>J. W. Negele, Phys. Rev. C **1**, 1260 (1970); H. Flocard, P. Quentin, A. K. Kerman, and D. Vautherin, Nucl. Phys. **A203**, 433 (1973).
- <sup>5</sup>P. Quentin and H. Flocard, Annu. Rev. Nucl. Sci. **28**, 523 (1978).
- <sup>6</sup>U. Mosel, P. G. Zint, and K. H. Passler, Nucl. Phys. **A236**, 252 (1974); U. Mosel, in *Heavy Ion Collisions*, edited by R. Bock (North-Holland, New York, 1980), Vol. 2, Chap. 4.
- <sup>7</sup>A. L. Goodman, in *Nuclear Theory 1981, Proceedings of the Nuclear Theory Summer Workshop, Santa Barbara, 1981*, edited by G. F. Bertsch (World Scientific, Singapore, 1982), pp. 255–296.
- <sup>8</sup>L. Moretto, Nucl. Phys. **A182**, 641 (1972).
- <sup>9</sup>A. K. Kerman and S. Levit, Phys. Rev. C **24**, 1029 (1981).
- <sup>10</sup>M. Brack and P. Quentin, Nucl. Phys. **A361**, 35 (1981).
- <sup>11</sup>O. Civitarese, A. L. De Paoli, and A. Plastino, Z. Phys. A **305**, 341 (1982); **309**, 177 (1982); **311**, 317 (1983).
- <sup>12</sup>M. Brack and P. Quentin, Phys. Lett. B **52**, 159 (1974); Phys. Scr. **A10**, 163 (1974).
- <sup>13</sup>S. Levit and Y. Alhassid, Nucl. Phys. **A413**, 439 (1984).
- <sup>14</sup>V. S. Ramamurthy, S. S. Kapoor, and S. K. Kataria, Phys. Rev. Lett. **25**, 386 (1970); for a review, see J. R. Huizenga and L. G. Moretto, Annu. Rev. Nucl. Sci. **22**, 427 (1972).
- <sup>15</sup>C. Chester, B. Friedman, and F. Ursell, Proc. Cambridge Philos. Soc. **53**, 599 (1957); M. V. Berry, Adv. Phys. **25**, 1 (1976).
- <sup>16</sup>S. Levit and U. Smilansky, Ann. Phys. (N.Y.) **108**, 165 (1977).
- <sup>17</sup>H. J. Lipkin, N. Meshkov, and A. J. Glick, Nucl. Phys. **62**, 188 (1965).
- <sup>18</sup>See, for example, N. Meshkov, A. J. Glick, and H. J. Lipkin, Nucl. Phys. **62**, 199 (1965); A. J. Glick, H. J. Lipkin, and N. Meshkov, *ibid.* **62**, 211 (1965); S. Levit, J. W. Negele, and Z. Paltiel, Phys. Rev. C **21**, 1603 (1980); Y. Alhassid and S. E. Koonin, *ibid.* **23**, 1590 (1981).
- <sup>19</sup>D. J. Thouless, Nucl. Phys. **22**, 78 (1961).
- <sup>20</sup>J. Des Cloizeaux, in *Many-Body Physics*, edited by C. de Witt and R. Balian (Gordon and Breach, New York, 1968), pp. 5–36.
- <sup>21</sup>R. Gilmore and D. H. Feng, Nucl. Phys. **A301**, 189 (1978); D. H. Feng, L. M. Narducci, and R. Gilmore, Proceedings of the International Conference on Frontiers of Physics, Singapore, 1978, pp. 1231–1270.
- <sup>22</sup>Y. Alhassid, N. Agmon, and R. D. Levine, Chem. Phys. Lett. **53**, 22 (1978).
- <sup>23</sup>This result was pointed out in a conversation with R. Balian.
- <sup>24</sup>When applying the mean-field approximation to a general many-body system it is more convenient to work with the grand-canonical thermodynamic potential  $\Omega = F + \mu N$  which depends also on the chemical potential  $\mu$ . The function  $\beta\Omega$  satisfies a stability property similar to  $\beta F$ , but with respect to fluctuations in both temperature and chemical potentials.
- <sup>25</sup>D. Agassi, H. J. Lipkin, and N. Meshkov, Nucl. Phys. **86**, 1321 (1966).
- <sup>26</sup>M. Abramowitz and I. A. Stegun, *Handbook of Mathematical Functions* (Dover, New York, 1965).
- <sup>27</sup>S. Levit (private communication).
- <sup>28</sup>R. Bellman, R. E. Kalaba, and J. A. Lockett, *Numerical Inversion of the Laplace Transform* (American Elsevier, New York, 1966).
- <sup>29</sup>A. Bohr and B. Mottelson, *Nuclear Structure* (Benjamin, New York, 1969), Vol. 1.
- <sup>30</sup>M. Brack and H. C. Pauli, Nucl. Phys. **A207**, 401 (1973).
- <sup>31</sup>O. S. van Roosmalen, F. Iachello, R. D. Levine, and A. E. L. Dieperink, J. Chem. Phys. **79**, 2515 (1983).